J. A. Viator, G. Paltauf, S. L. Jacques, S. A. Prahl, "Design and testing of an endoscopic photoacoustic probe for determining treatment depth after photodynamic therapy of esophageal cancer," in SPIE Proceedings of Biomedical Optoacoustics II, A. A. Oraevsky, 4256, 16-27, (2001).

Design and testing of an endoscopic photoacoustic probe for determination of treatment depth after photodynamic therapy

John A. Viator[a], Guenther Paltauf[b], Steven L. Jacques[c], and Scott A. Prahl[c]

[a]Beckman Laser Institute and Medical Clinic, 1002 Health Sciences Road East, Irvine, CA
[b]Karl-Franzens-Universitaet Graz, Graz, Austria
[c]Oregon Medical Laser Center, 9205 SW Barnes Road, Portland, OR

ABSTRACT

An endoscopic photoacoustic probe is designed and tested for use in PDT treatment of esophageal cancer. The probe, measuring less than 2.5 mm in diameter, was designed to fit within the lumen of an endoscope that will be inserted into an esophagous after PDT. PDT treatment results in a blanched, necrotic layer of cancerous tissue over a healthy, deeper layer of perfused tissue. The photoacoustic probe was designed to use acoustic propagation time to determine the thickness of the blanched surface of the esophagous, which corresponds to treatment depth. A side-firing 600 μm fiber delivered 532 nm laser light to induce acoustic waves in the perfused layer of the esophagous beneath the blanched (treated) layer. A PVDF transducer detected the induced acoustic waves and transmitted the signal to an oscilloscope. The probe was tested on clear and turbid tissue phantom layers over an optically absorbing dye solution.

Keywords: acoustic, propagation time, optical fiber, Nd:YAG, Q–switched, PVDF

1. INTRODUCTION

Photodynamic therapy (PDT) is a means of treating cancerous tumors by activating a drug which is preferentially absorbed or retained by the tumor. Drug activation is achieved by irradiating the tumor site, causing cell death in the tumor [1–8]. Currently, there is no means to evaluate the depth of treatment immediately following a PDT treatment in the esophagous. Knowledge of the treatment depth would aid the clinician in determining followup treatment, including the need for additional PDT procedures. This chapter describes the design, construction, testing, and use of a photoacoustic probe for use in determining treatment depth *in situ* immediately after the PDT treatment. This information may aid the clinician in deciding how to proceed with treatment of the tumor site.

1.1. Photodynamic Therapy for Esophageal Cancer

Esophageal cancer kills approximately 10,000 people per year [4]. The later stages of esophageal cancer are aggravated by dysphagia, weight loss, pain and fatigue. The dysphagia, or difficulty in swallowing, significantly decreases the patient's quality of life and is the chief aim of palliation. Additionally, palliation relieves pain and tumor bleeding. Treatment of esophageal cancer includes mechanical dilation of the esophagous, stenting, and surgical esophagectomy [4, 9, 10]. Mechanical dilation tends to be ineffective for other than short periods and may cause tissue trauma. Esophagectomy is a drastic surgical procedure. In 1996, the FDA approved the use of PDT in palliative treatment of obstructing esophageal cancer.

In a PDT case, the patient is intravenously given a photosensitive drug, such as porfimer sodium (Photofrin), which accumulates in the cancerous tissue. Approximately 48 hours later, an optical fiber is introduced within the esophagous via an endoscope. The optical fiber irradiates the tumor with approximately 300 J/ cm over 10–12 minutes. The temperature rise in the tissue due to the laser light is physiologically negligible. The light activated drug produces oxygen radical species in the tumor resulting in cell death. Upon light treatment, tissue blanching occurs due to the cessation of tissue perfusion, indicating the necrotic region of the treatment area. Photographs of the PDT treatment of an esophagous are shown in figure 1. The blanched areas indicate necrotic tumor tissue. The depth of necrosis should be equal to the blanched layer thickness, as indicated by the debridement of the tissue during the next 24 to 48 hours.

Further author information: (Send correspondence to J.A.V.)
J.A.V.: E-mail: javiator@laser.bli.uci.edu

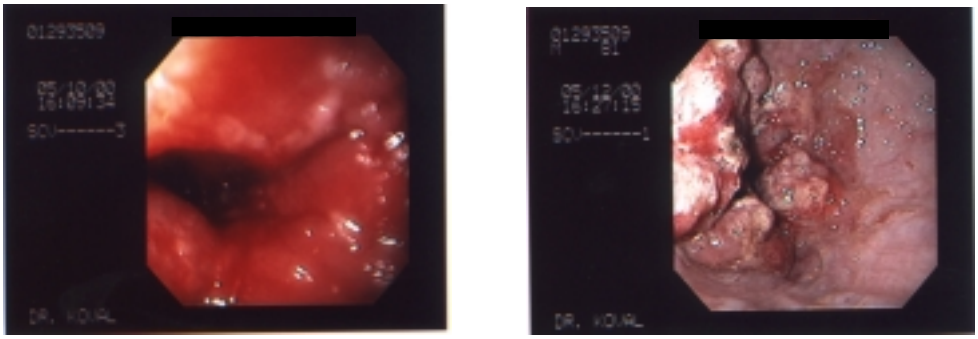

Figure 1. Photographs of the pre- and post-treatment esophagous. In the left photograph, the tumor area is shown as bulbous obstructions in the esophageal lumen. In the photograph on the right, the region of necrotic tissue is shown as a white, blanched area. The thickness of this blanched area indicates the depth of necrosis and hence, the depth of PDT treatment.

1.2. Photoacoustic Propagation Time

Photoacoustic propagation time has been used for locating positions of optical absorbers in tissue or tissue-like media. The key element in this type of scheme is that a known acoustic propagation time and sound speed will give an indication of the position of the acoustic source. This idea is at the heart of backprojection reconstruction. Esenaliev *et al.* [11] used propagation time methods to image deeply embedded tumor models in gelatin phantoms and to detect liver embedded in chicken breast. Viator *et al.* [12] used propagation time to detect small, optically absorbing spheres in turbid acrylamide gels. This paper uses simple propagation time analysis to determine the thickness of a turbid layer over an optically absorbing layer in order to model the blanched (necrotic) layer after PDT treatment in esophageal cancer.

A photoacoustic probe was designed that contained both a piezoelectric transducer, made from a polyvinylidenefluoride (PVDF) film, and a 600 μm optical fiber (figure 4). The optical fiber delivered stress confined laser pulses in a direction orthogonal to the axis of the fiber, while the PVDF film, located alongside the end of the side firing fiber, detected the resulting acoustic waves. The simple equation

$$d = c_s \tau \tag{1}$$

shows the relationship of the propagation time and sound speed to the source distance, where d denotes the distance from the transducer to the absorbing (perfused) layer, c_s is the speed of sound in the tissue, or tissue–like, medium, and τ is the time between the absorption of optical energy and the acoustic wave detection by the transducer. An artist's rendering of the use of the photoacoustic probe is shown in figure 2, where the probe is introduced to the esophagous via the working lumen of an endoscope. The probe comes into contact with blanched layers, where it irradiates the tissue and subsequently detects acoustic waves resulting from absorption in the deeper, perfused layer of esophagous. The probe was constructed and tested on clear and turbid layers over optically absorbing layers of various absorption coefficients. The probe needed to fit into the working lumen of an endoscope used in esophageal PDT. It needed to be sturdy, so as not to disintegrate within the esophagous and sensitive enough to detect blood perfusion in the healthy esophageal tissue underlying the blanched, necrotic layer.

2. MATERIALS AND METHODS

2.1. Photoacoustic Set Up

The set up for testing the photoacoustic probe is shown in figure 3. A Q–switched, frequency–doubled Nd:YAG laser (Quantel Brilliant, OPOTEK, Carlsbad, CA) operating at 532 nm launched 5 ns pulses into a 600 μm quartz optical fiber. The pulse repetition rate was 10 Hz. The pulse energy out of the laser was approximately 5 mJ. The pulse energy out of the fiber was approximately 2–2.5 mJ. The optical fiber was mode mixed by coiling the fiber.

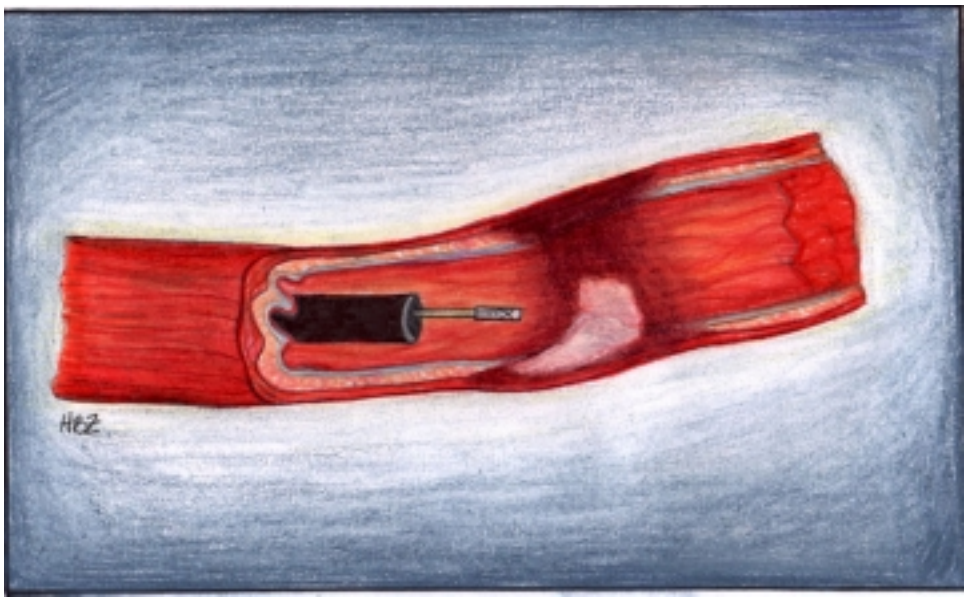

Figure 2. An artist's rendering of the use of the endoscopic photoacoustic probe. The probe emerges from the endoscope and is directed to treated (blanched) areas to determine the depth of necrosis.

The photoacoustic probe, described below, was attached to the end of the optical fiber. The probe was tested on various absorbing targets with the resulting acoustic signal being sent to an oscilloscope (DSA 602A, Tektronix, Wilsonville, OR). The bandwidth of the oscilloscope was 300 MHz with 1 Gsamples/s. The input impedance of the oscilloscope was 1 MΩ when the signal was not electronically amplified and 50Ω when the signal was amplified. For all experiments in which the target was submerged within a scattering solution, a background measurement was taken on pure scattering solution without any embedded absorber. This background measurement was subtracted from all subsequent measurements to acount for optical backscattering into the acoustic probe, resulting in an interfering pyroelectric signal, and to account for any absorption of the scattering solution itself.

2.2. Probe Construction

The photoacoustic probe was designed to couple an acoustic transducer to an optical fiber. The optical fiber delivered pulses of light from the Q–switched laser described previously in the set up. The acoustic transducer detected pressure signals resulting from the deposited laser energy. Both elements of the probe, the fiber and the transducer, were designed so that they would fit into the 2.8 mm working lumen of an endoscope used in the PDT procedure. The fiber/transducer pair were approximately 2.4 mm in diameter. The center to center distance from the fiber face to the acoustic detector was approximately 1100 μm. The optical fiber was polished at the distal fiber face at a 45° angle. This angled fiber face directed the laser energy orthogonally to the axis of propagation of the fiber. To ensure a glass/air interface for proper reflection at the 45° angled face, the fiber tip was encased in a glass tube and sealed. The acoustic transducer was coupled alongside the fiber and was side detecting, meaning that the active area was positioned to optimally detect pressure signals emanating from the direction of the deposited laser energy. The acoustic transducer design is shown in figure 4. The transducer was made from miniature coaxial cable (UT-34, Micro–Coax, Pottstown, PA) with a total diameter of 860 μm. The coaxial cable was composed of a center conductor, a dielectric, and a conducting shield. The shield of the coaxial cable was made from silver plated copper wire. The dielectric was made from polytetrafluoroethylene (PTFE). The center conductor was made from silver plated copper wire and had a diameter of 200 μm. The characteristic impedance was 50Ω. The capacitance was 95 pF/m.

A $7 \times 1\text{mm}^2$ sheet of 25 μm thick PVDF film, which had aluminum deposited on both sides, was connected to the center conductor by a small amount of conducting epoxy (CircuitWorks, Inc., Garland, TX). The top of the PVDF film was electrically coupled to the coaxial cable's outer shield with conducting epoxy. A photograph of the probe is shown in figure 5.

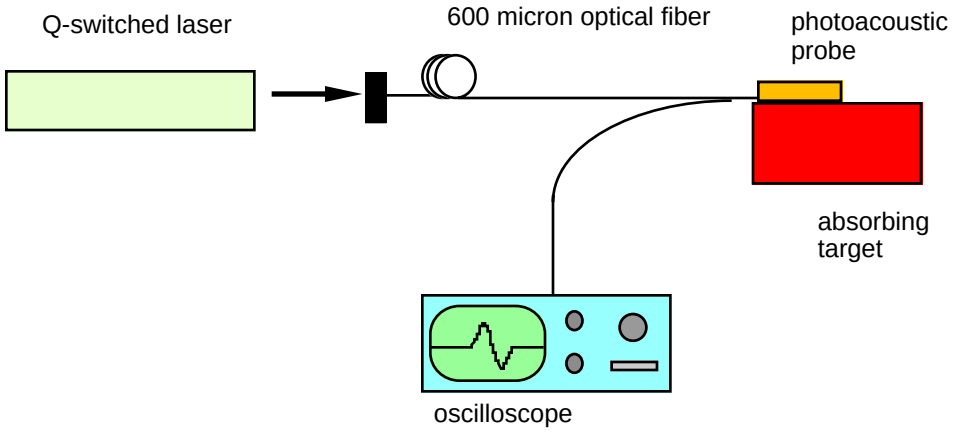

Figure 3. The Q–switched laser launched 532 nm, 5 ns pulses into a 600 μm fiber. A piezoelectric detector was positioned at the end of the optical fiber. Optically absorbing targets were irradiated by the fiber and the resulting acoustic waves were detected by the piezoelectric element. The signal was sent to the oscilloscope.

2.3. Amplification

A noninverting amplifier was built using a surface mount CLC425 ultra low noise, wideband operational amplifier (National Semiconductor, Arlington, TX). The gain–bandwidth product of the op amp was 1.9 GHz. Appropriate resistor values were used in the amplifier circuit to maintain a gain of 45. The circuit board was etched from a copper sheet over a plastic substrate. Conductive traces were designed to minimize RF noise.

2.4. Transducer Characteristics

The sensitivity of the acoustic transducer was characterized by irradiating Direct Red solutions of various absorption coefficients with 2.0 mJ of laser light in contact with the active area of the transducer. The relationship [13]

$$p(0) = \frac{1}{2}\Gamma\mu_a H_0 \tag{2}$$

where $p(0)$ is the pressure of the wave at the surface (point of detection), Γ is the Grüneisen coefficient, here assumed to be 0.12 [13], μ_a is the absorption coefficient of the solution and H_0 is the radiant exposure. The Direct Red solutions had absorption coefficients of 8, 16, 31, and 61 cm^{-1}. The spot sizes were approximately 1 mm in diameter. The radiant exposure was 0.064 $\mathrm{J/cm}^2$. This gave a temperature rise of less than 1°C, by the relation [14]

$$\Delta T = \frac{\mu_a H_0}{\rho C} \tag{3}$$

where ΔT is the change in temperature in degrees Celsius, and ρ is the density and C is the specific heat of the solutions.

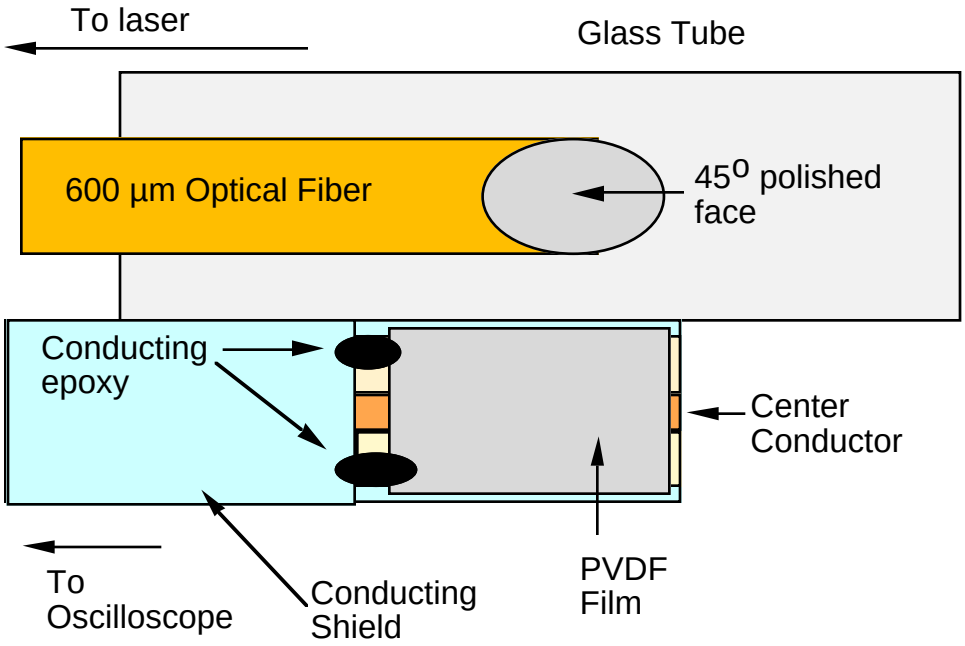

Figure 4. The photoacoustic probe is shown here. The 45° polished fiber face directed the laser light in a side firing mode (upwards, out of the plane of the page). The glass tube contained the fiber face and ensured a glass/air interface for proper reflection onto the target. The acoustic detector was positioned alongside the fiber. The detector was composed of a piezoelectric film on a miniature coaxial cable that sent the signal to the oscilloscope.

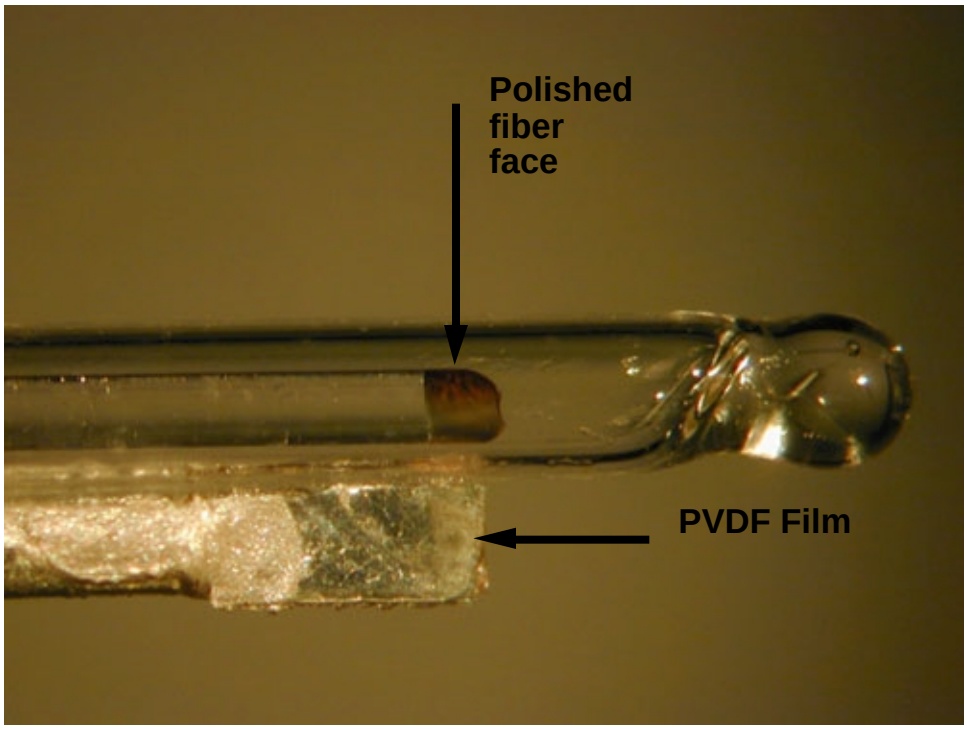

Figure 5. The photoacoustic probe is shown here. The total width of the fiber–detector pair is 2.4 mm. The glass tube is rounded at the tip to prevent damage to tissue.

2.5. Acoustic Testing

The photoacoustic probe was tested on tissue phantoms. These tissue phantoms were meant to simulate a necrotic, blanched layer of tissue over a perfused layer of esophagous. The phantoms were made with Direct Red 81 (Sigma Chemical, St. Louis, MO) in water. Four solutions were made with absorption coefficients of 8, 16, 30, and 61 cm^{-1} at 532 nm. Assuming an absorption coefficient of 300 cm^{-1} at 532 nm, these absorption coefficients correspond to 3, 6, 10, and 20% perfusion of tissue, respectively. The solutions were contained in a plastic circular cuvette 20 mm in diameter and 20 mm tall. Cuvettes containing distilled water or 1% Intralipid solutions (Liposyn, Abbott Laboratories, Abbott Park, Illinois) were placed above the cuvette with the red absorbing solution (figure 6). The 1% Intralipid solutions were used to simulate the reduced scattering coefficient of the blanched layer of esophagous, which was estimated at 15 cm^{-1} [15]. These cuvettes were 1–8 mm in height, in 1 mm increments. The photoacoustic probe was set in contact with the clear or turbid solutions. The detected acoustic waves were averaged over 32 pulses at a 10 Hz. The signal to noise ratio was calculated as a function of depth for the clear and turbid solutions. The noise was approximated by calculating the standard deviation of 50 points of a signal obtained from irradiating a phantom with no absorber. The noise value used was 2 mV. The signal amplitude was calculated by the peak height of the acoustic signal.

3. RESULTS

3.1. Transducer Characteristics

The acoustic transducer had a sensitivity of 1.5 mV/bar. The amplifier circuit had an electronic gain of 40, so that amplified signals would have a sensitivity of 60.0 mV/bar.

3.2. Acoustic Testing

The results of the acoustic testing are shown in this section. A montage of the acoustic waveforms for the 60 cm^{-1} absorbing solutions are displayed, with the clear intervening layers in figure 7 and the turbid intervening layers in figure 8. The depths of intervening layers are 1–8 mm in 1 mm increments. The acoustic wave delay was approximately

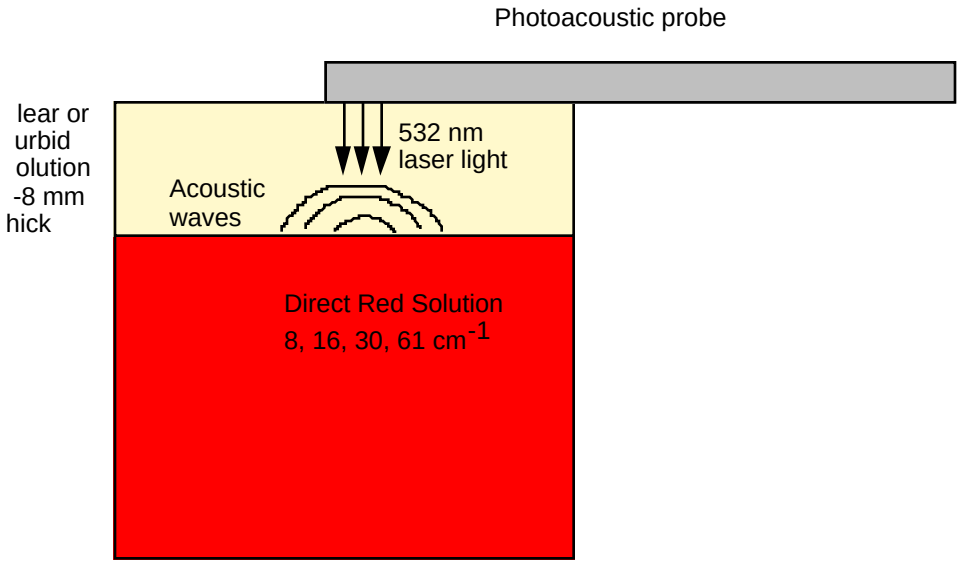

Figure 6. The acoustic testing of the photoacoustic probe was performed by irradiating solutions of various absorption coefficients under clear or turbid solutions of various thicknesses. The resulting acoustic waves were detected by the photoacoustic probe and sent to an oscilloscope.

0.7 μs between graphs, though a small meniscus contributed to measurement error. The meniscus was approximately 1 mm. For a 1 mm intervening layer, this accounts for 50% of the acoustic delay, though at 8 mm, it only accounts for a 13% of the acoustic delay.

The signal to noise ratios for all four absorption coefficient solutions as a function of depth with clear and turbid intervening layers are shown in figure 9 and figure 10, respectively.

4. DISCUSSION

4.1. Photoacoustic Propagation Time

The concept of propagation time is simple, assuming a constant sound speed to calculate a distance based on the time of arrival of an acoustic wave. The assumption of sound speed in tissue-like media as 1.5 mm/μs is valid for water, milk, fat, nerve tissue, muscle, etc [16]. The situation for a post–treatment esophagous, however, is aggravated by the complex geometry caused by uneven uptake of photosensitizer, treatment light distribution, or other factors. These factors, though not affecting sound speed, would change the propagation path, making the distance calculation inaccurate. The geometry of the post–treatment esophagous may not be planar, nor even a reasonable approximation of one. Repeated measurements and systematic scans may smooth these inhomogenous effects by integrating the bumps in an otherwise smooth heating distribution which creates the photoacoustic field.

4.2. Acoustic Testing

The results of the acoustic wave generation in the 8, 16, 31, and 61 cm^{-1} absorption coefficient solutions with clear intervening layers showed signal to noise (SNR) ratios as high as 150. In the 16, 31 and 61 cm^{-1} solutions, the SNR was greatest for the 3 and 4 mm layers. The 8 cm^{-1} solutions were much lower than the others. The greatest SNR occurring at 3 or 4 mm is explained by the fact that at 1 and 2 mm, the PVDF film is not directly over the laser spot, as the distance from the fiber to spot is comparable to the separation distance of the fiber and the PVDF film (figure 11). The drop off in SNR after 4 mm is due to decrease in radiant exposure, due to spot size increase and acoustic attenuation. The SNR's shown in the turbid layers didn't show the high SNR behavior at 3 or 4 mm since the light was diffuse, causing the laser spots to be larger and encompassing the region below the fiber and detector.

The turbid solutions were a better model of the esophagous, as the blanched layer in the post-treatment esophagous is scattering. Assuming a whole blood optical absorption of 300 cm^{-1} at 532 nm, the 8, 16, 31, and 61 cm^{-1} solutions

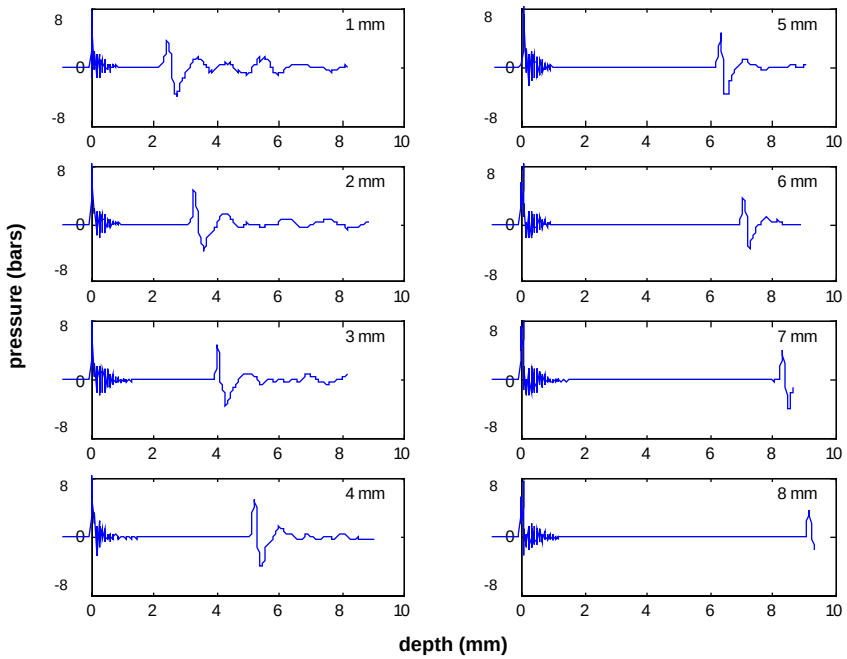

Figure 7. The acoustic waves resulting from irradiating a Direct Red solution ($\mu_a = 60\,\mathrm{cm}^{-1}$) with various thicknesses (1–8 mm) of clear water between the absorbing solution and the detector. The signal, easily discernable from the noise level, was delayed as the clear layers become thicker. Zero on the horizontal axis indicates the laser pulse trigger.

represented perfusions of 3, 5, 10, and 20%, respectively. A perfusion of 5–10% is reasonable for elevated perfusion levels in cancerous tissue, so detection of perfused layers in the esophagous may occur in as deep as 7-8 mm, with an SNR of 4 or higher, neglected other factors such as high background absorption or nonplanar geometry. Even with a 3% perfusion, detection may occur to 4 or 5 mm.

ACKNOWLEDGMENTS

We wish to thank Halina Brant-Zawadzki for her excellent medical illustration. We also thank Christian Sturges and David Spain for their assistance in the probe construction.

REFERENCES

1. S. Heier, K. Rothman, L. Heier, and W. Rosenthal, "Photodynamic therapy for obstructing esophageal cancer: Light dosimetry and randomized comparison with nd:yag laser therapy," *Gastroenterology* **109**, pp. 63–72, 1995.
2. J. M. Jr., E. C. Ellison, J. Guy, W. Hicks, J. Jones, L. Laufman, E. May, T. Nims, C. H. Spiridonidis, and T. Williams, "Photodynamic therapy for esophageal malignancy: A prospective twelve-year study," *Ann. Thoracic Surgery* **62**, pp. 1005–1010, 1996.
3. C. Lightdale, S. Heier, N. Marcon, J. M. Jr., H. Vgerdes, B. Overholt, M. S. andG. Stiegmann, and H. Nava, "Photodynamic therapy with porfimer sodium versus thermal ablation therapy with nd:yag laser for palliation of esophageal cancer: A multicenter randomized trial," *Gastrointestinal Endoscopy* **42**, pp. 507–512, 1995.
4. S. B. Narayan and M. V. S. Jr., "Palliation of esophageal carcinoma," *Chest Surg. Clinics of N. Am.* **4**, pp. 347–367, 1994.
5. A. L. Abramson, M. J. Shikowitz, V. M. Mullooly, B. M. Steinberg, C. A. Amella, and H. R. Rothstein, "Clinical effects of photodynamic therapy on recurrent laryngeal papillomas," *Arch. Otolaryngol. Head Neck Surg.* **118**, pp. 25–29, 1992.

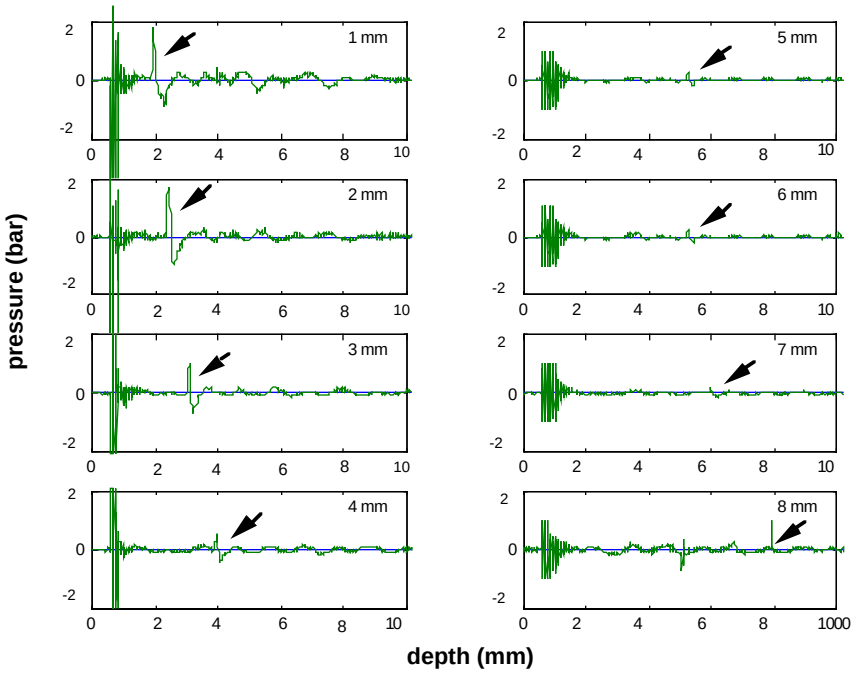

Figure 8. The acoustic waves resulting from irradiating a Direct Red solution ($\mu_a = 60\,\mathrm{cm}^{-1}$) with various thicknesses (1–8 mm) of turbid solution ($\mu_s' = 15\,\mathrm{cm}^{-1}$) between the absorbing solution and the detector. The signal, easily discernable from the noise level, was delayed as the turbid layers become thicker.

6. J. Moan and K. Berg, "Photochemotherapy of cancer: experimental research," *Photochemistry and Photobiology* **55**, pp. 931–948, 1992.
7. A. D. Nguyen, "Photodynamic therapy with porfimer sodium (photofrin)," *Highlights in Oncology Practice* **15**, pp. 21–24, 1997.
8. H. I. Pass, "Photodynamic therapy in oncology: Mechanisms and clinical use," *J. Nat. Cancer Inst.* **85**, pp. 443–456.
9. M. B. Orringer, B. Marshall, and M. D. Iannettoni, "Transhiatal esophagectomy: clinical experience and refinements," *Ann. of Surg.* **3**, pp. 392–403.
10. M. G. Patti, C. U. Corvera, R. E. Glasgow, and L. W. Way, "A hospital's annual rate of esophagectomy influences the operative mortality," *J. of Gastrointestinal Surg.* **2**, pp. 186–192, 1998.
11. R. O. Esenaliev, A. A. Karabutov, and A. A. Oraevsky, "Sensitivity of laser opto–acoustic imaging in detection of small deeply embedded tumors," *IEEE J. Sel. Topics Quant. Electron.* **5**, pp. 981–988, 1999.
12. J. A. Viator, S. L. Jacques, and S. A. Prahl, "Depth profiling of absorbing soft materials using photoacoustic methods," *IEEE J. Sel. Topics Quant. Electron.* **5**, pp. 989–996, 1999.
13. G. Paltauf, H. Schmidt-Kloiber, and H. Guss, "Light distribution measurements in absorbing materials by optical detection of laser-induced stress waves," *Appl. Phys. Lett.* **69**, pp. 1526–1528, 1996.
14. J. A. Viator and S. A. Prahl, "Laser thrombolysis using long pulse frequency–doubled nd:yag lasers," *Lasers in Surg. and Med.* **25**, pp. 379–388, 1999.
15. S. T. Flock, S. L. Jacques, B. C. Wilson, W. M. Star, and M. J. C. van Gemert, "Optical properties of intralipid: A phantom medium for light propagation studies," *Lasers in Surg. and Med.* **12**, pp. 510–519, 1992.
16. F. A. Duck, *Physical Properties of Tissue*, Academic Press, 1990.

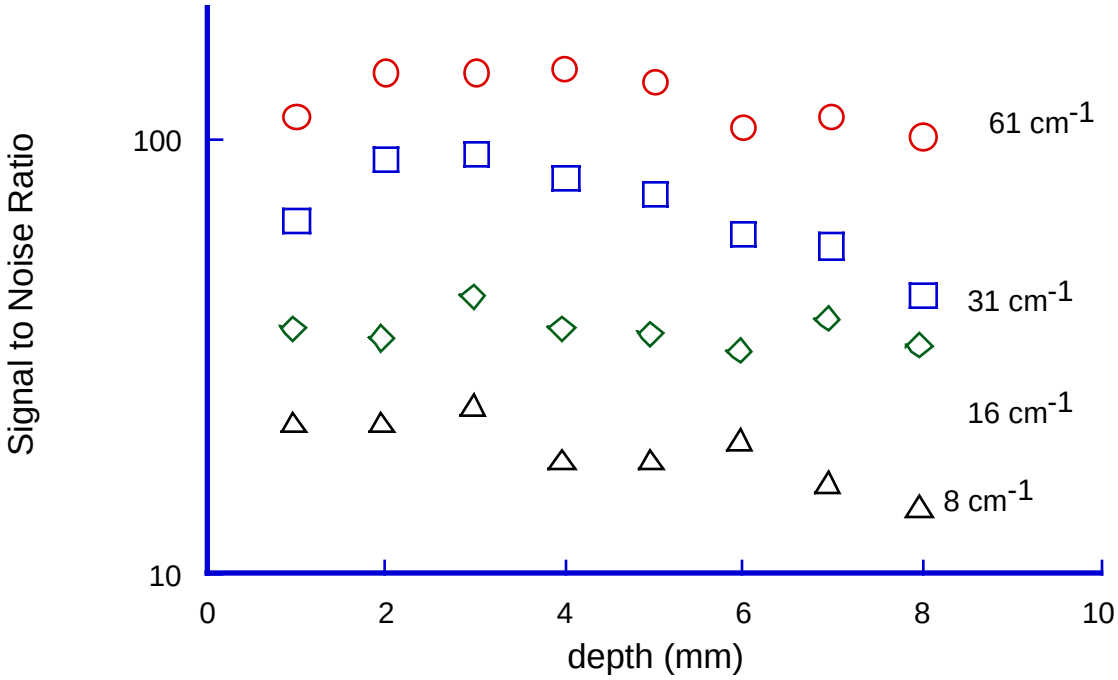

Figure 9. The signal to noise ratios for the solutions of various absorption coefficient are shown as a function of depth of clear layer. The maximum signal occurred at 3–4 mm of depth, due to the offset of the acoustic detector from the optical fiber. This offset caused the acoustic wave source to be not directly underneath the detector, decreasing the detector sensitivity. The acoustic signal maximized at about 3–4 mm away, as the resultant larger spot created acoustic waves directly beneath the detector. For greater than 4 mm, the lower radiant exposure dominated the the acoustic signal generation, resulting in a weaker acoustic detection.

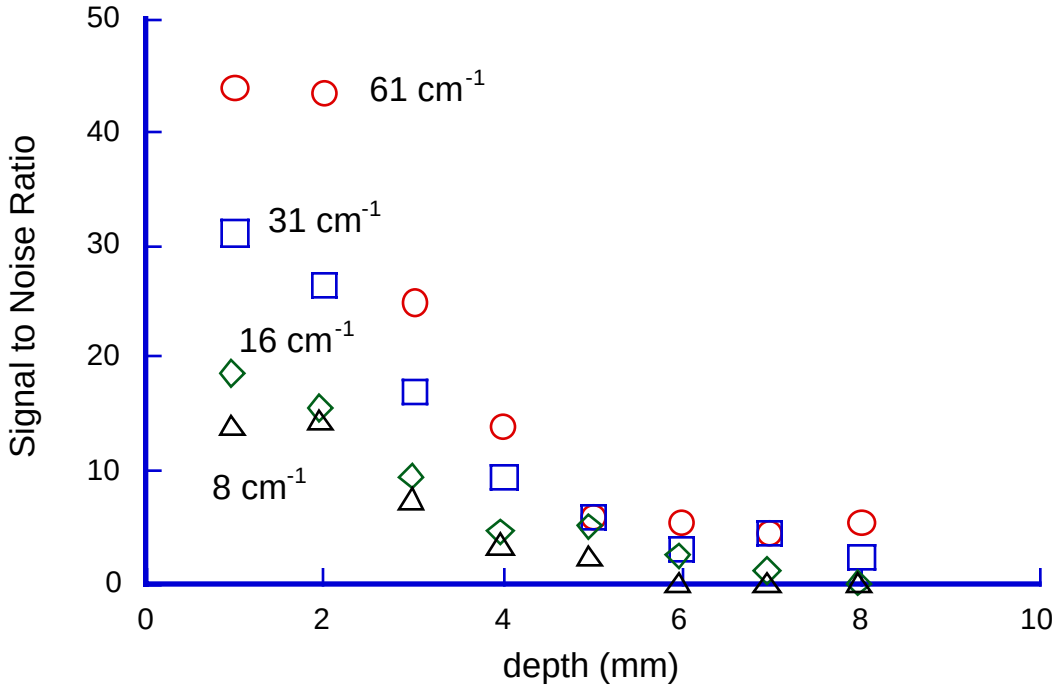

Figure 10. The signal to noise ratios for the solutions of various absorption coefficient are shown as a function of depth of turbid layer. The maximum signal occurred at 1 mm, as the highest radiant exposure occurred and optical diffusion was stronger at greater distances, decreasing the acoustic signal strength.

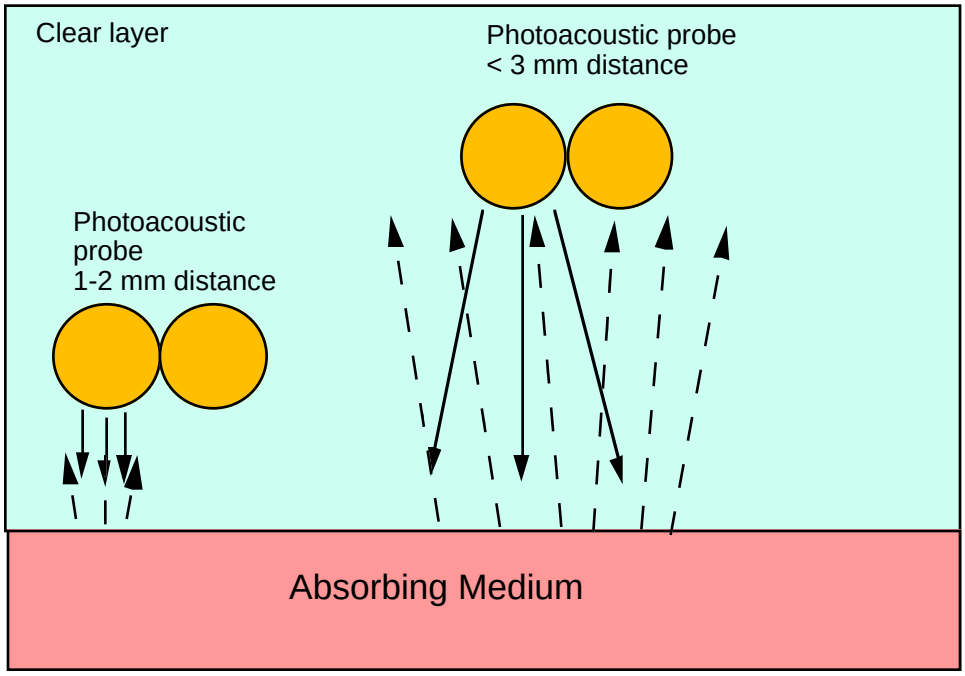

Figure 11. For the clear intervening layer, the acoustic signal for distances of 1-2 mm is weaker than signals detected at 3-5 mm, as the acoustic sensor is not directly over the acoustic source when the probe is so close. This is due to the antenna function of the probe and the small spot size. After about 5 mm, the decreased radiant exposure results in a weaker acoustic wave, making the detected signal weaker.